Transport in Advanced Scenarios on ASDEX Upgrade

A.G. Peeters, A. Bergmann, G.D. Conway, H. Meister, G.V. Pereverzev, G. Tardini,
O. Gruber, M. Manso†, F. Serra†, R.C. Wolf

MPI für Plasmaphysik, D-85748 Garching, Germany, EURATOM-Association
† CNF, IST Lisboa 1096 Portugal, EURATOM association

e-mail contact of main author: Arthur.Peeters@ipp.mpg.de

Abstract Detailed studies of the confinement physics in advanced scenarios on ASDEX Upgrade are presented. The confinement of the improved H-mode can largely be unified with that of the standard H-mode. The increase in the H-factor is partly due to density peaking, partly due to the density dependence in the scaling law, and partly due to the non-thermal population if a non-corrected scaling law is used. The confinement region of these discharges can be simulated well with the ITG/TEM models. Clear transport barriers are observed to be formed in discharges with reversed shear. Turbulence suppression is observed in these discharges, and within the error bars this is in agreement with the $E \times B$ paradigm. Monte Carlo simulations of the neoclassical transport in discharges with reversed shear show a reduction compared to the standard theory, and agree reasonably well with the experimental ion heat conductivity over a large inner region.

1. The improved H-mode

The record value of $n_{D0} T_{i0} \tau_E = 9 \cdot 10^{19}$ keV·s·m^{-3} ($\beta_N = 2.4$ $H_{\mathrm{ITER89-P}} = 3.0$) on ASDEX Upgrade is obtained in the improved H-mode [1,2]. This regime is obtained through pre-heating in the current ramp up phase, but with smaller power than the L-mode ITBs. The power is increased at the end of the current ramp up phase, causing a transition into the H-mode, and a stationary state is obtained.

Detailed studies have shown that the physics picture of the confinement in this regime of operation can be largely unified with that of the standard H-mode. In Fig. 1 the data of a density scan $0.3 < n/n_{\mathrm{Greenwald}} < 0.6$ is shown. The discharges in this scan have the same plasma current (1 MA), the same NBI heating power (5 MW), and low triangularity $\delta < 0.25$. The color coding is explained in the figure. The following observations can be made: The shots with pre-heating have in general a low line averaged density and a high central and edge ion temperature. The few standard shots that also have high temperatures are special shots which are tailored to have a low edge density and allow for a check of the hypothesis described in this paper. The ion temperature profile is stiff (the central value is a factor times the value at $r = 0.8a$, with r being the volume radius). The electron temperature deviates from the linear dependence at lower density (higher temperature) where the electron-ion coupling is reduced. The density profiles peak at lower density and show a steep increase of peaking at a line average density around $4 \cdot 10^{19}$ m^{-3}, correlated with the flattening of the electron temperature.

The roughly constant pressure at the pedestal top allows for a high ion edge temperature when the edge density is low. Due to the stiffness also the core temperature increases. This explains the high ion core temperatures of the improved H-mode, but would not lead to an increase in the stored energy if the density profile would be stiff as well. The density peaking at low line averaged densities, however, leads to such an increase. The H-factor, the relative improvement of the confinement time τ_E over the scaling ITER98(y,1), shown in Fig. 1 has some scatter but a fit allows to estimate the increase over the studied density range to be a factor 1.62. A part of the

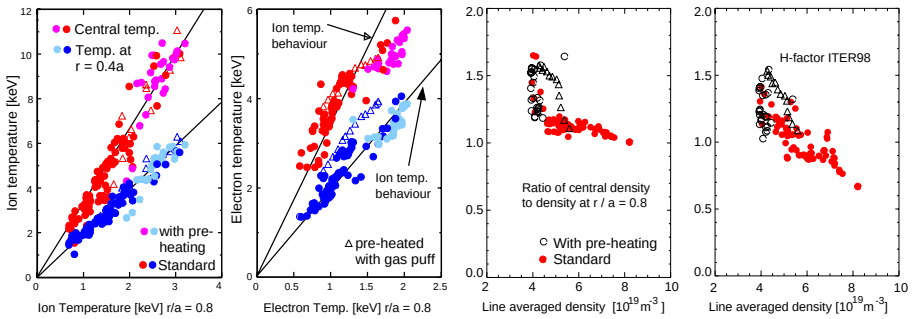

Figure 1: *Comparison of improved H-mode with standard H-mode*

improvement can be thought to be due to the density dependence in the scaling law $\tau_E \propto \overline{n}_e^{0.41}$ which would not occur in the physics picture discussed above. If the confinement time of the experiment is independent of the density then a relative improvement against the scaling law is obtained if one goes to lower density. This can explain an increase in H-factor of 36%, which is somewhat too low to explain the entire increase. The additional improvement in the H-factor is expected to be due to the density peaking. Indeed, integrating the obtained density profiles with a standard ion temperature profile gives an estimate of the increase in stored ion energy due to the density peaking alone of 32%. For the electrons the density peaking and flattening of the electron temperature profile partly compensate each other yielding only a small increase in stored energy. So the density peaking has a clear favorable effect. It is however difficult to calculate the stored energy directly from the profiles because of the uncertainty in the determination of Z_{eff} and the contributions to it from the various elements. Simply integrating the profiles assuming $n_i = n_e$ yields an increase of 70% in stored ion energy, but Z_{eff} is observed to go up at lower densities, and partly reduces the ion density and therefore the ion stored energy. The standard discharges with low density show that as far as confinement is concerned the pre-heating is not essential. The improved H-mode can better be defined through the density peaking.

The ion and electron temperatures profiles in the outer region $0.4a < r < 0.8a$ can successfully be modeled [3] with the ITG/TEM models of Weiland [4] (shown in blue in Fig. 2), and IFS-PPPL [5] (shown in red). These models predict stiff ion temperature profiles in agreement with the experimental observations. The IFS-PPPL model slightly over-predicts the gradient length ($E \times B$ shear is included in all models). Weiland predicts this quantity better on average but there is also more scatter. It must be noted too that the non-stiff behavior of the electrons is also reasonably predicted by these models. The instability is dominantly driven by the ion temperature gradient and the flattening of the electron profile is related to the reduced energy coupling, with

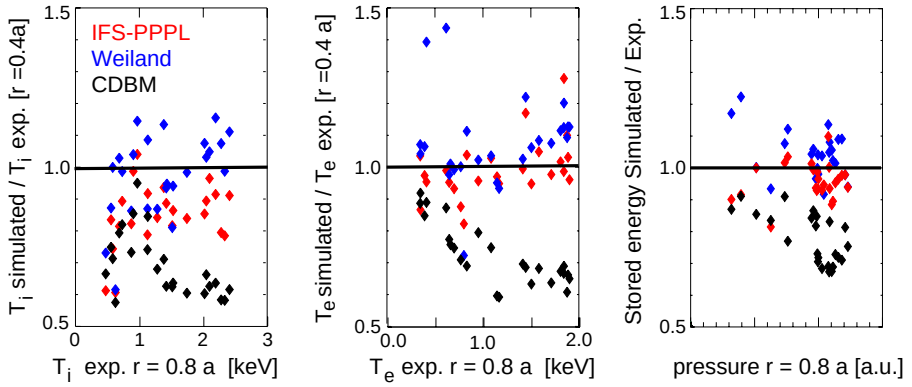

Figure 2: *Results of theory based transport simulations*

less power going into the electrons at lower density. The profiles can not be explained very well by the non-stiff CDBM model [6] shown in black. The standard deviation of predicted stored energy over the measured stored energy for the different models is: $\sigma_{\mathrm{IFS-PPPL}} = 9.5\%$, $\sigma_{\mathrm{Weiland}} = 9.2\%$, and $\sigma_{\mathrm{CDBM}} = 24.1\%$. A deviation of 9% is better than obtained with the scaling law. However, the boudary condition for the temperature (applied at r = 0.8a) as well as the density profile is taken from the experiment, i.e. a better prediction can be expected.

2. Internal Transport barriers

Most of the ITBs on ASDEX Upgrade are obtained through significant heating, usually around 5 MW, in the current ramp up phase, and preventing the H-mode through a limiter configuration or unfavorable drift direction. Transiently the magnetic shear is reversed in the center, and ITBs form with the ion temperature gradient length being much smaller than that of the H or L-mode. This is shown in Fig. 3 where the different confinement regimes are compared. The large scatter in the ITB data suggests non-stiff behavior or different confinement states.

It has been found that the Shafranov shift in the reversed shear discharges plays an important role in bringing down the growth rates to levels where they are below the $E \times B$ shearing rate. The central Shafranov shift is much larger than in normal discharges because of the large safety factor on axis, connected with the negative shear. Fig. 3 shows the growth rates obtained from the GLF23 model [7] of two discharges (#12224 without ECRH shown in blue and #12229 with ECRH shown in red) together with the shearing rates for comparison. In the discharge with ECRH, which is described in detail in [8,9], the electron temperature could be raised to 10 keV without any change in the ion temperature. The growth rates in the first plot which are calculated without Shafranov shift show that raising the ratio of electron to ion temperature is destabilizing for the ITG. This destabilizing effect, however, is largely compensated by the stabilizing Shafranov shift which is larger in the case with ECRH because the electron pressure in the center is raised.

The shearing rates shown in Fig. 3 are obtained assuming neoclassical poloidal rotation, which might not be entirely justified since corrections to the standard theory are expected as will be discussed below. The shearing rate from the measured poloidal rotation is in general larger, but it must be noted that the error bars on these measurements are rather large leading to significant uncertainties. In the discharges with internal transport barriers the turbulence is observed to be suppressed. This is shown in Fig. 4 which shows the reflectometry signals as a function of time for discharge #13553. Around $t = 0.75$ a clear reduction of the turbulence is observed. At this

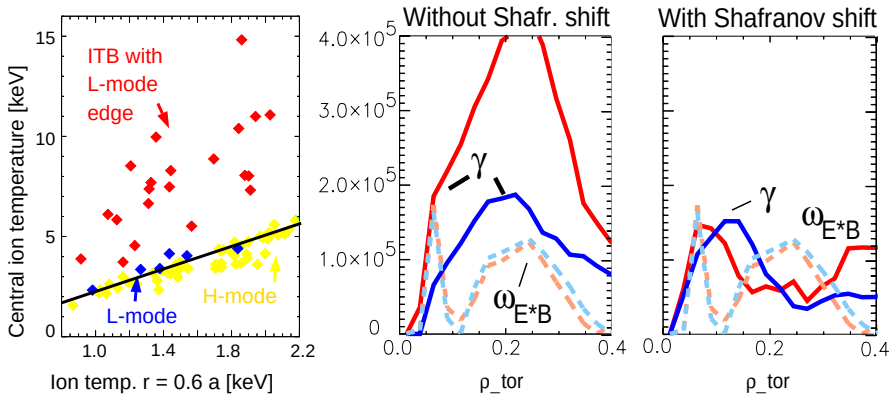

Figure 3: *Ion temperature peaking, Growth and shearing rates of the ITB with L-mode edge*

time point the position of the reflection layer falls together with the foot of the transport barrier $\rho \approx 0.6a$. Using the neoclassical poloidal rotation yields shearing rates which are somewhat too small to explain the suppression of the anomalous transport at this location. Unfortunately, the poloidal rotation was not measured in this shot. However, the comparison of the shearing rate obtained from the measured poloidal rotation with the linear growth rate for a different discharge #13149 (which has slightly larger temperatures) shows that the shearing rate largely exceeds the growth rates in the center of the discharge and is of the same order as the growth rate at the foot of the barrier ($\rho = 0.6a$) [10]. Within the error bars the assumption that the $E \times B$ shearing rate suppresses turbulence is in agreement with the experiment. The uncertainty in the measurement, however, does not allow for a stronger statement at the present time.

3. Neoclassical transport close to the axis

If the $E \times B$ shear suppresses the turbulence on scale lengths several times the ion gyro radius, for which the reflectometry is sensitive, than the ion heat transport is expected to be reduced to the neoclassical level. In many experiments it has in fact been found to lie below standard neoclassical theory. Standard neoclassical theory indeed breaks down close to the axis because the radial size of the orbits is no longer small compared with the minor radius of the flux surface. Fat banana orbits, so called potato orbits are formed with a radius r_p

$$r_p = 1.6(2q\rho)^{2/3}R^{1/3}$$

where q is the safety factor, ρ is the gyro radius, and R is the major radius. Especially in reversed shear discharges this radius, and consequently the region in which the standard theory breaks down, can be large.

Different theories [11,12], with strong contradicting results, try to describe the influence of the large orbits on the neo-classical ion heat flux. The theory of Z. Lin predicts a strong decrease in the heat flux, whereas the theory of Shaing gives a heat flux even larger than the standard theory. To investigate this discrepancy, and to compare the transport in the L-mode ITBs of ASDEX Upgrade with neoclassical theory Monte Carlo δf simulations have been performed. The δf code integrates the particle orbits in Boozer coordinates. A Monte Carlo procedure is used to model the collisions, which consist of pitch angle scattering and a correction for momentum conservation. More details of the applied method can be found in Ref. [13].

Fig. 5 shows the results of these calculations. The figure on the left shows the obtained ion heat conductivity normalized to the thin orbit theory as a function of the radius normalized to the potato width. Different simulations are shown which have been obtained by varying

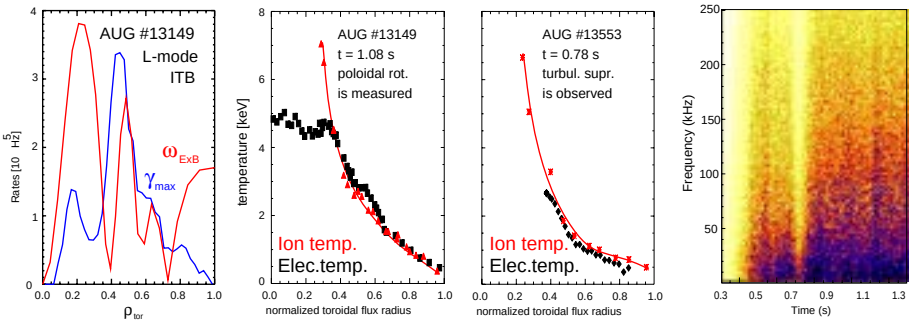

Figure 4: *Observed suppression of turbulence.*

$0.05 < r_p/a < 0.15$, through a variation in q and R, in a circular equilibrium. It can be seen that the different simulations yield roughly the same result in normalized units For $r \gg r_p$ the results of the standard theory are obtained. Also shown are the predictions of the afore mentioned theories. The reduction of the transport is in qualitative agreement with the theory of Lin, but the heat fluxes for $r < r_p$ are much larger. It must be mentioned here that the comparison is with the analytic formula of Lin, and not a direct comparison with his code results. The difference in the range $r < r_p$ is important for the comparison with the experiment. In the figure on the right the experimental and simulated heat conductivity of an ASDEX Upgrade discharge (#10701) with an ITB and H-mode edge is shown. The simulations are done for a real ASDEX Upgrade equilibrium, correcting for Z_{eff} with a multiplication factor. Reasonable agreement is obtained over a large range including the region of the steep gradient around $r/a = 0.5$. This gives strong support to the assumed switch off of the anomalous ion heat transport.

Acknowledgment The authors of the theory based transport models are acknowledged for providing the computer codes containing the models.

References

[1] GRUBER O. et al., Phys. Rev. Lett. **83** (1999) 1787.

[2] WOLF R. et al., Plasma Phys. Contrl. Fusion **41** (1999) B93.

[3] TARDINI G. et al., The proceedings of the 27th EPS conference (Budapest 2000).

[4] NORDMAN, H., et al., Nuclear Fusion **30** (1990) 983.

[5] KOTSCHENREUTHER M. et al., Phys. Plasmas **2** (1995) 2381.

[6] ITOH S.-I et al., Plasma Phys. Control. Fusion **38** (1996) 1743.

[7] WALTZ R.E., et al., Phys. Plasmas **4** (1997) 863.

[8] GÜNTER S., et al., Phys. Rev. Lett. **84** (2000) 3097.

[9] WOLF R.C., et al., Phys. Plasmas **7** (2000) 1839.

[10] MEISTER H. et al., to appear in Nuclear Fusion (2000)

[11] LIN Z. et al., Phys. Plasmas **4** (1997) 1404.

[12] SHAING K.C. et al., Phys. Plasmas **4** (1997) 771.

[13] BERGMANN A. et al., The proceedings of the 27th EPS conference (Budapest 2000).

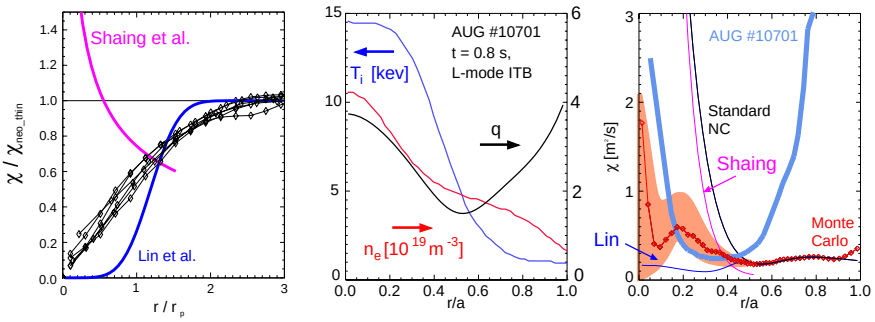

Figure 5: *Result of Monte Carlo delta-f calculations*